Title

DHA-SBT-1214 Taxoid Nanoemulsion and Anti–PD-L1 Antibody Combination Therapy Enhances Antitumor Efficacy in a Syngeneic Pancreatic Adenocarcinoma Model

Journal

Molecular Cancer Therapeutics, 18(11)

ISSN

1535-7163

Authors

Ahmad, Gulzar
Mackenzie, Gerardo G
Egan, James
et al.

Publication Date

2019-11-01

DOI

10.1158/1535-7163.mct-18-1046

Peer reviewed

DHA-SBT-1214 Taxoid Nanoemulsion and Anti-PD-L1 Antibody Combination Therapy Enhances Anti-Tumor Efficacy in a Syngeneic Pancreatic Adenocarcinoma Model

Gulzar Ahmad[1], Gerardo G. Mackenzie[2], James Egan[3], and Mansoor Amiji[1,4]

[1] Department of Pharmaceutical Sciences, School of Pharmacy, Northeastern University, Boston, Massachusetts, 02115-5000.
[2] Department of Nutrition, University of California at Davis, 3135 Meyer Hall, Davis, CA 95616
[3] Targagenix, Inc., 25 Health Sciences Drive, Stony Brook, New York, 11790-3382.

[4]Corresponding author: Mansoor Amiji, PhD, Department of Pharmaceutical Sciences, School of Pharmacy, Northeastern University, Boston, Massachusetts 02115. Phone: 617-373-3137; Fax: 617-373-8886; E-mail: m.amiji@northeastern.edu

Running head: Combination chemo- and immuno-therapy in pancreatic adenocarcinoma.
Conflict of interest: The authors declare that they have no conflicts.

Keywords: DHA-SBT-1214 taxoid nanoemulsion, anti-PD-L1 antibody, combination therapy, pancreatic adenocarcinoma.

ABBREVIATIONS: Multidrug Resistance (MDR), Docosahexaenoic Acid (DHA), Poly(Ethylene Glycol) (PEG), Dulbecco's Modified Eagle's medium (DMEM), 1, 2-Distearoyl-Sn-glycero-3-Phospho Ethanolamine-N-[amino [Poly(Ethylene Glycol)-2000] (DSPE-PEG2000), Transmission Electron Microscopy (TEM), Limulus Amebocyte Lysate (LAL), High Performance Liquid Chromatography (HPLC), Institutional Animal Care and Use Committee (IACUC), Paclitaxel (PTX), Area Under the Curve (AUC), Polydispersity Index (PDI). Overall Patient Survival (OS), Programmed Death Ligand-1 (PD-L1), Programmed Death-1 (PD-1), Mouse Pancreatic Adenocarcinoma Cell line (Panc02), Gemcitabine (GEM), Myeloid Derived Suppressor Cells (MDSC).

Novelty and Impact: Combination of a novel taxoid DHA-SBT-1214 with anti-PD-L1 immune check point inhibitor for improved therapeutic efficacy in a syngeneic mouse model of pancreatic cancer.

ABSTRACT

The goal of this study was evaluate combination of a novel taxoid, DHA-SBT-1214 chemotherapy in modulating immune checkpoint marker expression and ultimately in improving antibody-based checkpoint blockade therapy in pancreatic adenocarcinoma (PDAC). DHA-SBT-1214 was encapsulated in an oil-in-water nanoemulsion and administered systemically in Panc02 syngeneic PDAC-bearing C57BL/6 mice. Following treatment with DHA-SBT-1214, PD-L1 expression levels were measured and anti-PD-L1 antibody was administered in combination. The effects of combination therapy on efficacy and the molecular basis of synergistic effects were evaluated. Panc02 pancreatic tumor cells expressed low levels of PD-L1 in vitro, which significantly increased after exposure to different chemotherapy drugs. Administration of DHA-SBT-1214, gemcitabine and PD-L1 antibody alone failed to increase $CD8^+$ T-cell infiltration inside tumor. However, combination of anti-PD-L1 therapy with a novel chemotherapy drug DHA-SBT-1214 in nanoemulsion (NE-DHA-SBT-1214), significantly enhanced $CD8^+$ T-cell infiltration and the therapeutic effects of the anti-PD-L1 antibody. Furthermore, in Panc02 syngeneic model, NE-DHA-SBT-1214 combination therapy group reduced tumor growth to higher extend than paclitaxel, nab-paclitaxel (Abraxane^{TM}), gemcitabine, or single anti-PD-L1 antibody therapy groups. Our results suggest that NE-DHA-SBT-1214 stimulated immunogenic potential of PDAC and provided synergistic therapeutic effect with immune checkpoint blockade therapy, which warrants further evaluation.

INTRODUCTION

In the United States, pancreatic adenocarcinoma (PDAC) is currently the fourth leading cause of cancer-related deaths and is projected to rise significantly in the next decade largely due to an increase in type I and II diabetes epidemic [1]. The current standard of care in pancreatic cancer includes surgery, radiation and chemotherapy [2]. The high mortality associated with PDAC is attributed mainly to advanced stage diagnosis and therapeutic resistance to agents, such as gemcitabine [2, 3]. In advanced stage PDAC, especially when the tumor has metastasized to other parts of the body, systemic chemotherapy with gemcitabine and taxanes, is the most important interventional option. However, these chemotherapeutic drugs lack tumor specificity and are highly prone to the development of multi-drug resistance (MDR) [4]. Instead of gemcitabine chemotherapy alone, the combination with nab-paclitaxel (Abraxane^{TM}), and a cocktail of 5-fluorouracil, oxaliplatin, irinotecan, and leucovorin (FOLFIRINOX) have shown better results in patients' overall survival (OS) response [5]. Along with toxicity issues, one of the major limitations of chemotherapy agents in PDAC is their inability to penetrate the highly fibrotic and desmoplastic tumor tissue, thereby limiting the effectiveness to the rapidly proliferating PDAC cells confined to the tumor periphery [2]. This inefficiency of current therapies explains, in part, the lower success rate of anticancer drug development for PDAC and other solid tumors [6].

As such, there is an urgent unmet need to develop safer and more effective therapeutic strategies that can improve on PDAC's dismal OS. Over the last several years, we have developed next generation taxoids that show superior antitumor efficacy, especially in refractory tumors by targeting the cancer initiating (or stem) cell population. One of these next generation taxoids, SBT-1214 has shown superior efficacy against a highly drug-resistant (Pgp+) colon tumor xenograft in SCID mice [7]. In another study, SBT-1214 completely suppressed the tumor

recurrence [8]. To further improve the tumor specificity and decrease systemic toxicity, we have conjugated SBT-1214 with docosahexaenoic acid (DHA), an omega-3 polyunsaturated fatty acid [9]. Previously, we have evaluated the efficacy of DHA-SBT-1214 in colon, ovarian, pancreatic and non-small cell lung tumor xenografts in mouse models and demonstrated improved efficiency as compared all the other control studies [10].

Due to poor aqueous solubility and susceptibility of the ester bond in DHA-SBT-1214 to cleave in the presence of esterases in the systemic circulation, we have formulated the drug in omega-3 fish oil-rich nanoemulsion formulation. In a previous studies, we have observed that nanoemulsion encapsulated DHA-SBT-1214 (NE-DHA-SBT-1214) shows improved delivery efficiency, tumor residence, improved therapeutic efficacy, and less systemic toxicity in a subcutaneous stem cell-rich PPT-2 human prostate tumor xenograft model [11].

Use of cancer immunotherapy agents, such as blocking the immune checkpoint inhibition and new cell therapies that enhance the effectiveness of cytotoxic T-cells, have become major breakthroughs in the treatment of solid tumors [12, 13]. Although immunotherapy with immune check point inhibitors have shown significant preclinical and clinical efficacy in many different types of tumors, the overall efficacy in PDAC is limited [14]. Among immune check point inhibitors, programmed death-ligand 1 (PD-L1) on tumor cells binds with programmed death-1 (PD-1), which is found on activated T-cells and a member of the CD28 family and sends an inhibitory signal to T-cell and stops immune response [13, 15]. One of the early immune-oncology agent approvals in the United States is nivolumab (Opdivo®), a fully humanized IgG4 PD-1 antibody, which restores anticancer immune responses by abrogating PD-1 pathway-mediated T-cell inhibition and has been approved for use in the United States for treating patients with unresectable melanoma [13, 15, 16], non-small cell lung cancer [15] and renal cell carcinoma [17]. In

addition to anti-PD-1 and anti-PD-L1, various other immune checkpoint inhibitors, including antibodies against CTLA-4 are approved and being used in combination for many solid tumor types [18-20]. In murine preclinical pancreatic cancer models, anti-PD-1 or anti-PD-L1 antibodies have shown better antitumor effect [14, 21]. Due to highly variable expression of PD-L1 in human pancreatic cancer, no studies to date have demonstrated the clinical efficacy of immune checkpoint inhibitor monotherapy for PDAC [22]. Although anti-CTLA-4 drug ipilimumab (Yervoy®) in combination with a cancer vaccine has shown marginal survival benefit in clinical patients with pancreatic cancer [23, 24].

One of the limitations of immunotherapy in PDAC could be due to dense and highly fibrotic tumor stroma that prevents antibodies and T-cell infiltration into the tumor mass. As such, in order for an immunotherapy treatment to be effective in PDAC, it would need to be combined with antifibrotic agents and other small molecule or immune-based therapies to make the tumors responsive to immunotherapy. In this regard, very few studies have addressed the PD-1/PD-L1 pathways, with some showing contradictory findings [25-28]. In this study, we have investigated how anticancer agents (paclitaxel, gemcitabine, Abraxane™ and DHA-SBT-1214) influence PD-L1 expression in PDAC model. As such, combination of a small molecule chemotherapy along with an antibody against check point inhibitor would have synergistic effect for PDAC treatment. Additionally, we provide evidence that NE-DHA-SBT-1214 in combination with PD-L1 antibody shows improved anticancer effect due to higher penetration of CD8 T-cells inside the tumor.

MATERIALS AND METHODS

Materials

Docosahexaenoic acid conjugate of SBT-1214 (i.e., DHA-SBT-1214) was synthesized by ChemMaster International, Inc. (Stony Brook, NY) following the previously reported method [7, 29, 30]. Extra pure grade omega-3 rich fish oil was purchased from Jedwards International (Quincy, MA), Lipoid E80 from Lipoid GMBH (Ludwigshafen, Germany), DSPE PEG2000 from Avanti Polar Lipids, Inc. (Alabaster, AL), Tween 80 from Sigma Chemicals, Inc. (St. Louis, MO), Dulbecco's Modified Eagle Medium (DMEM) and LAL chromogenic endotoxin quantitation kit from Thermo Scientific (Rockford, IL). Penicillin, streptomycin and trypsin were obtained from Invitrogen (Grand Island, NY, USA). Female C57BL/6 mice (4-6 weeks old) were purchased from Charles River Laboratories (Frederick Research Model Facility-NCI) (Cambridge, MA, USA). Amicon Ultra-0.5ml, Centrifugal filters from Millipore (Cork, Ireland). All other analytical grade reagents were purchased through Fisher Scientific. In the present study, we used Gemcitabine (GEM), paclitaxel (PTX) and Abraxane™ which are agents commonly used to treat pancreatic cancer; all agents were immediately prepared before use. GEM and PTX were purchased from Sigma Chemicals, Inc. (St. Louis, MO).

Preparation and Characterization of DHA-SBT-1214 Nanoemulsion Formulations

Preparation of blank and DHA-SBT-1214 encapsulated fish oil/water nanoemulsion formulations was carried out with a well-established protocol as reported recently with some modifications [11, 31-33]. Instead of the sonication method, oil-in-water nanoemulsions were prepared by high pressure homogenization method. The formulations were characterized for oil droplet size, surface charge, drug encapsulation efficiency, and the morphology of the oil droplets was evaluated with transmission electron microscopy.

Cell Culture

The murine pancreatic cancer cell line Panc02, which is syngeneic to C57Bl/6 mice was kindly provided by Professor Michael Hollingsworth from the University of Nebraska Medical Center (Omaha, NE) [34]. Panc02 cells were grown in 75 cm^2 cell culture flasks and maintained in DMEM medium supplemented with 10% fetal bovine serum (FBS), L-glutamine and penicillin (100 U/ml)/streptomycin (100 μg/ml) (both from Gibco Life Technologies, Carlsbad, CA, USA). Cells were incubated at 37°C in a humidified atmosphere containing 5% CO_2.

In Vitro Evaluations of Nanoemulsion Uptake and Cellular Distribution

Panc02 cells ($0.5x10^6$) were seeded onto glass cover-slips in 6-well plates for overnight at 37°C in a humidified atmosphere containing 5% CO2. Then cells were incubated with 2 μM of rhodamine administered in nanoemulsion for different time points ranging from 0.5 h to 4 h to allow uptake of nanoparticles by cells. After last incubation time point, the glass cover-slips were washed with PBS before fixing in formalin for 15 minutes at room temperature. Nuclei of the fixed cells were stained with 4', 6-diamidino-2-phenylindole (DAPI). Uptake of rhodamine nanoemulsion was studied by a fluorescence confocal microscope (Zeiss LSM 700) with fixed parameters to have comparable uptake among different time points.

Cell Viability Studies

To see cytotoxic effect of different drugs and nanoemulsion formulation, 5000 cells were seeded in each well of the 96-well plate for overnight at 37°C in a humidified atmosphere containing 5% CO2. Various control and test treatments (i.e., paclitaxel solution, Abraxane™, gemcitabine solution, and solution and nanoemulsion of DHA-SBT-1214) were diluted at

concentrations ranging from 0 nM, 0.01 nM, 0.1 nM, 1 nM, 10 nM, 100 nM, 1000 nM to 10000 nM and Panc02 cells treated with these concentrations for 96 hours. After incubation, cells were treated with 3-(4,5-dimethylthiazol-2-yl)-2,5-diphenyltetrazolium bromide (MTT). MTT crystals were dissolved with DMSO and plates were read at 570nm absorbance using a BioTek Synergy HTX Multi-Mode Microplate Reader.

Expression of PD-L1 after Exposure to Different Therapeutic Agents

Cells were seeded at $0.5x10^6$ cells/well in 6-well plates for overnight at 37℃ in a humidified atmosphere containing 5% CO2. After 24 hours, cells were exposed to IC_{50} value of different drug treatments as described in Figure 2 for 48 hours. The expression level of PD-L1 was determined using flow cytometry as follows. Briefly, cells harvested from *in vitro* cultures were washed twice with 3% BSA/PBS and then incubated with rat anti-PD-L1 or isotype control antibodies (mouse, BioXcell, West Lebanon, NH, USA) for 30 min at 4^oC. After washing three times, the cells were incubated with anti-rat AlexaFluor 488 conjugated antibody. The cells were again washed once with 3% BSA/PBS and analyzed by flow cytometer on a FACSCalibur flow cytometer and CellQuest™ Pro version 6.0 software (both from Becton-Dickinson and Co.).

Immunoblotting

Cells and tumor tissues were washed twice with phosphate-buffered saline (PBS) and lysed in ice-cold lysis buffer containing 2% proteinase inhibitor (both from Sigma-Aldrich Company, St. Louis, MO, USA). Cells were retrieved with a cell scraper, stirred and incubated on ice for 15 min, whereas, mice tumor tissues were sonicated for 10 seconds on ice with an ultrasound probe. Lysates were centrifuged, supernatants were collected, and protein

concentration was determined using the Bio-Rad protein assay (Bio-Rad Laboratories, Hercules, CA, USA). The supernatants were diluted with lysis buffer to create equal concentrations of protein. Fifty micrograms of protein were separated on 4-12% Bis-Tris gels and transferred onto a nitrocellulose membrane using the iBlot Dry Blotting System (all from Life Technologies) according to the manufacturer's protocol. Blots were blocked with 1% dry milk in TBS-T [10 mM Tris-HCl (pH 8.0), 150 mM NaCl, 0.1% (v/v) Tween-20] for 1 hour at room temperature and washed once with TBS-T. The membranes were incubated overnight at 4°C with anti-PD-L1 ((ab58810), from Abcam), PD-1 ((D7D5W) XP® Rabbit mAb, 84651S), F4/80 ((D2S9R) XP® Rabbit mAb, 70076S) and Histone 3 ((D1H2) XP® Rabbit mAb, 4499S), (all from Cell Signaling Technology, Inc.) antibodies in TBS-T (diluted 1:1,000). After washing in TBS-T three times, the membranes were incubated with the secondary anti-rabbit and mouse IgG antibodies (Life Technologies) in TBS-T (diluted 1:10,000) for 1 h at room temperature. Immunocomplexes were detected using western blotting (ECL Prime; GE Healthcare UK Ltd., Buckinghamshire, UK).

Quantitative Polymerase Chain Reaction (qPCR)

The expression level of PD-L1 and mRNA for other proteins was determined using real-time PCR. The samples used for mRNA isolation were removed from the pancreatic cancer cells (Pan02) or tumor tissues. Total mRNA was extracted using commercially available RNA extraction kit according to mentioned protocol (Thermo Fisher Scientific (Rockford, IL). The isolated RNA was stored at -80˚C until use for real-time qPCR. In the latter, 1 µg of extracted RNA was reverse-transcribed using commercial cDNA synthesis kit (Thermo Fisher Scientific (Rockford, IL). The resulting cDNA was subjected to RT-PCR with Applied Biosystems™

PowerUp™ SYBR™ Green Master Mix (Thermo Fisher Scientific (Rockford, IL), using the following primers for mouse PD-L1: (forward primer, 5'-AAAGTCAATGCCCCATACCG-3' and reverse primer, 5'-TTCTCTTCCCACTCACGGGT-3')[35] ; mouse PD-1 (forward primer, 5'-TTCACCTGCAGCTTGTCCAA-3' and reverse primer, 5'- TGGGCAGCTGTATGATCTGG-3')[35] ; CD4: (forward primer, 5'- ACACACCTGTGCAAGAAGCA-3' and reverse primer, 5'-GCT CTTGTTGGTTGGGAATC-3')[36] ; mouse CD8 (forward primer, 5'- CTCACCT GTGCACCCTACC-3' and reverse primer, 5'-ATCCGGTCCCCTTCACTG-3')[36] ; mouse Arginase-1 (forward primer, 5'-GAACACGGCAGTGGCTTTAAC -3' and reverse primer, 5'-TGCTTAGCTCTGTCTGCTTTGC-3')[37] ; and mouse β-actin (forward primer, 5'-CTCCTGAGCGCAAGTACTCTGTG-3' and reverse primer, 5'-TAAAACGCAGCTCAGTAACAGTCC-3')[38]. PCR was performed using a real-time PCR system (7300; Applied Biosystems, Foster City, CA, US A). Relative quantifications of gene expression with qRT-PCR data were calculated relative to murine β-actin as a housekeeping control.

In Vivo Studies – Subcutaneous Tumor Inoculation and Growth

All experiments involving the use of animals were carried out in strict accordance with the recommendations in the guide for the Care and Use of Laboratory Animals published by the National Institutes of Health. The protocol for animal experiments was approved by Northeastern University's Institutional Animal Care and Use Committee (IACUC). Briefly, after sufficient propagation, Panc02 murine pancreatic cancer cells were resuspended in 1:1 PBS/Matrigel and 2×10^5 cells injected subcutaneously to the right flanks of a 6 weeks old C57Bl/6 mice. Tumor development was monitored twice weekly. The tumor size was measured with a caliper on a

weekly basis and approximate tumor volumes determined using the formula $0.5ab^2$, where b is the smaller of the two perpendicular diameters. The mice were sacrificed when the tumor volume reached $\geq 1{,}500\ mm^3$ in diameter.

In Vivo Single and Combination Therapies

Mouse antibody against PD-L1 (10F.9G2) and relevant isotype IgG control was purchased from Bio X Cell. Two hundred micrograms of antibody against PD-L1 and relevant isotype IgG control was injected through i.p. per mice twice a week for 3 weeks. Gemcitabine solution and Abraxane™ at 120mg/kg was injected through i.p. once a week. Paclitaxel 120mg/kg and NE-DHA-SBT-1214 either 10mg/kg or 25mg/kg was injected once a week through i.v. All chemotherapy drugs were either injected in combination to anti PD-L1 antibody or isotype IgG control. In total, three treatments were given per experiment.

Histology and Immunohistochemistry (IHC) Analysis of Tumor Tissues

Histological analysis of tumor burden in mice was done on formaldehyde-fixed and paraffin-embedded tumor tissues using hematoxylin and eosin (H&E) staining. IHC was done on paraffin-embedded tissue sections for PD-1 ((D7D5W) XP® Rabbit mAb, 84651T), CD4 ((D7D2Z) Rabbit mAb, 25229T) and CD8 ((D4W2Z) XP® Rabbit mAb, 98941T) antibodies (Cell signaling technology, Danvers, MA). IHC was processed according to the protocol and recommended dilution from Cell Signaling Technology.

Data Analysis and Statistics

All results are expressed as the means ± SD. For therapeutic experiments, three mice were assigned per treatment group. Statistical analysis was performed with GraphPad Prism 6 software. Data were analyzed using unpaired Student's t test, and ANOVA and its differences were considered to be statistically significant at $p < 0.05$.

RESULTS

Characterization of DHA-SBT-1214 Nanoemulsion Formulation

Nanoemulsion delivery approach has shown enhanced therapeutic potential in our previous studies [11, 33]. In this study, we formulated an oil-in-water nanoemulsion of DHA-SBT-1214, a new-generation taxoid using fish oil, which is rich in PUFAs such as omega-3 and omega-6 fatty acids. We used a high pressure homogenization technique to formulate this uniform, milky-white and stable nanoemulsion [39]. As shown in Figure 1, the nanoemulsion droplets were near spherical in morphology with an average diameter of approximately 220 nm, as observed by light scattering and transmission electron microscopy (TEM). Along with particle size, uniformity and charge of the nanoemulsions also predicts their bioavailability. Uniformity of droplet size in a sample is represented by polydispersity index (PDI) and the lower value of PDI (<0.2) indicates uniform and stable form of nanoemulsions. PDI values of drug encapsulated nanoemulsions were less than 0.1. The average surface charge of the oil droplets in the nanoemulsions was -28.9 mV (Figure 1c). The negative charge of the nanoemulsion could be due to the presence of free fatty acids of the fish oil used in the preparation of these nanoemulsions.

An HPLC assay was used to determine the drug concentrations in the nanoemulsion formulations. DHA-SBT-1214 nanoemulsion at 20 mg/ml represents drug loading efficiency of 97%. All the formulations were filtered through 0.2-micron filter and had a minimum level of

endotoxin as confirmed through Limulus Amebocyte Lysate (LAL) assay during the storage period.

In Vitro Evaluations of DHA-SBT-1214 Formulations in Panc02 cells

To examine whether nanoemulsions were internalized in Panc02 cells, rhodamine was encapsulated into nanoemulsions and confocal microscopy studies were performed. The optimal cell and spheroid uptake of rhodamine encapsulated nanoemulsion formulation was observed after rhodamine 2 µM incubation at different time points (Figure 1d). As shown in Figure 1d, the images clearly depict that the nanoemulsions do efficiently deliver the encapsulated dye in the cells and that the increased fluorescence signal at increased time points of rhodamine nanoemulsion treated cells indicates the higher intracellular uptake by Panc02 cells. Since the internalization of nanoemulsion formulation was confirmed by cell uptake experiments, we replaced rhodamine with DHA-SBT-1214 in the nanoemulsion formulation and compared its effect on cell viability with different anti-cancer drugs.

The cell-kill efficiency of different anti-cancer drugs was examined in Panc02 cells using the MTT assay. In addition to blank nanoemulsion or vehicle control, the final concentrations of DHA-SBT-1214 selected for these studies were 0.01 nM, 0.1 nM, 1 nM, 10 nM, 100 nM, 1,000 nM to 10,000 nM based on previous studies of SBT-1214 [4]. The concentration-response studies against DHA-SBT-1214 and other anticancer agents in Panc02 cells are shown in Figure 2. The results are shown as percent viable cells remaining as a function of treatment following 96 hours of drug exposure at 37ºC. When DHA-SBT-1214 was administered at 10 and 100 nM concentrations, higher cytotoxicity was observed with the nanoemulsion formulation as compared to the aqueous solution. However, under in vitro conditions, gemcitabine showed

highest potency with average IC_{50} value of 154 nM, followed by 215 nM for DHA-SBT-1214 nanoemulsion and 262 nM for DHA-SBT-1214 in solution. In contrast, the average IC_{50} values of paclitaxel and Abraxane™ were significantly higher than DHA-SBT-1214, at 443 nM and 428 nM, respectively.

Evaluation of PD-L1 Expression Following Drug Therapy in Panc02 Cells

Panc02 cells were treated with gemcitabine, nab-paclitaxel (Abraxane™), paclitaxel and DHA-SBT-1214 both in solution and nanoemulsion for 48 hours to determine whether they can induce PD-L1 protein expression. PD-L1 expression levels on tumor cells were determined by flow cytometry and is expressed as the Δ mean fluorescence intensity (ΔMFI; MFI using anti-PD-L1 subtracted from the isotype control). As shown in Figure S1a, treatment with different anticancer drugs at their IC_{50} values for 48 h induced PD-L1 surface expression in Panc02 murine pancreatic cancer cells. PD-L1 upregulation in response to the anticancer agents tested was significantly increased compared to the untreated control. As reported previously, PD-L1 level enhanced in pancreatic tumor tissues compared to *in vitro* growing cells as shown in Figure S1b[40, 41].

***In Vivo* Evaluation of Combination Drug and anti-PD-L1 Antibody Therapy**

We have examined the effect of different anticancer agents either alone or in combination to blocking antibody against PD-L1 on Panc02 induced tumor growth in vivo. Panc02 cells were directly injected into subcutaneously and tumor volumes were measured one week later and continued till the end of the experiment. After tumor size reaches approximately 100 mm^3, we randomized the mice to have approximately equal tumor volume among all treatment groups.

Then, mice were treated with either anticancer agents either alone or in combination to PD-L1 antibody for three weeks. Figures 3a, b, c, and d, show the tumor growth inhibitory effects of each treatment group after the three week-treatment. As compared with the untreated control group, each treatment group had inhibitory effect which was most prominent in 25mg/kg NE-DHA-SBT-1214 in both IgG and PD-L1 antibody combination treated groups. These results indicate that blocking of only PD-L1 was not efficient in reducing tumor growth but in combination with 25mg/kg NE-DHA-SBT-1214 significantly inhibited tumor growth. NE-DHA-SBT-1214 treatment even at 10mg/kg in combination to PD-L1 antibody was more effective in suppressing tumor growth compared to standard chemotherapy drug, gemcitabine. Treatment with 10mg/kg DHA-SBT-1214 was superior to Abraxane^{TM} treatment at 120 mg/kg. Overall, a combinational treatment of NE-DHA-SBT-1214 with anti-PD-L1 antibody showed a synergistic effect compared with single treatment, and this was particular noticeable for in particular for NE-DHA-SBT-1214 10 mg/kg plus PD-L1, compared to NE-DHA-SBT-1214 plus IgG. As a crude proxy for acute toxicity of the treatment protocols, we evaluated the changes in body weight. As shown in Supplementary Figure 4. there was no significant body weight change within each treatment group.

Anticancer Drugs Induce PD-L1 Expression *In Vivo* in Panc02 Tumor Model

To investigate how the anticancer agents, induce PD-L1, PD-1, CD4, CD8 and Arginase-1 mRNA expression in pancreatic tumor tissues, the mRNA level of PD-L1, PD-1, CD4, CD8 and Arginase-1either alone or in combination of immune checkpoint inhibitor was determined by RT-PCR. PD-L1 mRNA level was upregulated in combination therapy among all the anticancer agents compared to their respective IgG control groups as shown in figure 4a. However, CD4

and PD-1 mRNA level was lower in anti- PD-L1 plus anticancer agents except gemcitabine which was not significantly higher compared to its IgG treated group as shown in Figure S2a and S2c respectively. CD8 mRNA level was upregulated in response to combination treatment of all anticancer agents when combined with immune check point inhibitor compared to their IgG treated groups as shown in Figure S2b respectively. However, Arginase-1 level was significantly higher in IgG treatment group compared to their immune check point inhibitor as described in Figure S2d. In addition to upregulation of PD-L1 mRNA expression level, treatment of anticancer agents in combination to immune check point inhibitor also enhance PD-L1 protein expression level as shown in Figure 4b and c. Similar to PD-L1 protein expression, PD-1 expression was also up-regulated except higher dose of NE-DHA-SBT-1214 compared to its IgG treatment group. Higher PD-L1 protein level might be attributed to presence of macrophages in this higher dose NE-DHA-SBT-1214 treated group which is evident due to higher protein level of F4/80 in Figure 4b and c.

Infiltration of CD4+, CD8+, and PD-1 Cells in Panc02 Tumor

We examined the infiltration of CD4+, CD8+, and PD-1 cells in tumor tissues at the end of experiment by histology (Figure 5) and by immunohistochemistry (Figure 6a and 3S a, b and c). The tumor tissue histology from different treatment groups showed that tumor from NE-DHA-SBT-1214 treated group has less dense stroma compared to solid tumor mass from other treatment groups (Figure 5).

In untreated control tumor tissues, a relatively small number of CD4+ cells were found. As compared to the untreated tumors, infiltration of CD4+ cells was significantly increased by

anti-PD-L1 treatment and with different anticancer agents combination treatments (Figure 6a and Supplementary Figure 3a).

Only a small number of CD8+ cell infiltrations were observed in control tumor tissue. Treatment with anti-PD-L1 antibody in combination with NE-DHA-SBT-1214 resulted in a significant increase of CD8+ cell infiltration in tumor microenvironment (Figure 6b and Supplementary Figure 3b). The infiltration of CD8+ cells in the core of pancreatic tumor is probably responsible for the suppression of tumor growth in each of the different treatment groups. However, expression of PD-1 on the T-cells was comparable among all treatment groups (Figure 6c and Supplementary Figure 3c).

DISCUSSION

Pancreatic cancer remains an intractable disease due to development of resistance to conventional anticancer agents. Currently, there is a great enthusiasm for immunotherapy in many treatment regimens due to the success of immune checkpoint inhibitors and new generations of adoptive cell transfer therapy, such as chimeric antigen receptor (CAR) T-cell therapy [42]. However, immune checkpoint inhibitors have not shown promising results when used as a single treatment regimen in many tumor types, especially in certain solid tumors, such as PDAC. As such, there are extensive efforts toward effectively combining immune- and non-immune based cancer therapies with the aim of improving response rate and efficacy.

For PDAC patients, gemcitabine is currently used as a frontline treatment in combination with Abraxane^{TM}; however, the survival benefit is minimal. Paclitaxel is still a front-line treatment for many other solid tumor types [43, 44] as it initiates the apoptosis and causes cell cycle arrest at the G_2/M stage [45, 46]. However, some cancers including colon and prostate overexpress

P-glycoprotein (Pgp), an effective ATP-binding cassette (ABC) transporter and actively effluxes paclitaxel from the cell, the drug is not effective [4]. In order to overcome the Pgp efflux issues, paclitaxel has been conjugated with DHA and the conjugated drug was found to have higher affinity for human serum albumin, which is also the primary carrier for PUFAs in the bloodstream [10]. However, when paclitaxel is cleaved by esterases from the DHA conjugate in the systemic circulation, the free drug is still susceptible to efflux by Pgp and other ABC transporters in tumors [10].

In contrast to paclitaxel, a new-generation taxoid, named SBT-1214, has shown excellent activity against drug-resistant cancer cells, which express MDR phenotypes, including Pgp [4, 8, 10]. In previous studies, DHA-conjugated SBT-1214 improved therapeutic efficacy by increased accumulation of drug at the tumor site through the enhanced permeability and retention effect [39]. To further improve the efficacy of DHA-SBT-1214, we successfully formulated and studied the nanoemulsion carrier system containing DHA-SBT-1214 in fish oil droplets, which favorably acted as drug reservoir. This colloidal system has desired particle size and zeta potential to preserve the stability of formulation in vitro and enhance its performance *in vivo* [47]. The surface morphology DHA-SBT-1214 nanoemulsion formulation was spherical in morphology with no visible drug crystals. The qualitative cellular uptake analysis demonstrated that the nanoemulsion formulations were efficiently internalized in Panc02 cells. This suggests that the nanoemulsions did efficiently deliver the payload to the subcellular sites in the cell and was more potent than its drug solution. In our recent study [11], we observed that DHA-SBT-1214 suppressed tumor growth to a higher extent when delivered in nanoemulsion formulations emphasizing its higher therapeutic efficacy when used as stand-alone therapy. Our data from the previous study demonstrated that nanoemulsion of the DHA-SBT-1214 conjugate induces superior regression

and tumor growth inhibition and has high potential as a novel anti-cancer drug candidate [11]. In the current study, we have explored the efficacy of the combination of immune therapy and anticancer agents in pancreatic cancer. As reported previously, PD-L1 surface expression in pancreatic cancer cell lines Panc02 was upregulated by paclitaxel, Abraxane^{TM}, DHA-SBT-1214 and gemcitabine.

To the best of our knowledge, this is the first study to address the effect of anticancer agents in combination to check point inhibitor on PD-L1 expression in a syngeneic pancreatic cancer mouse model. Although the effect of chemotherapy agents on PD-L1 expression has been discussed in previous studies, there have been conflicting findings [25-28]. For instance, three studies demonstrated that anticancer agents upregulated surface PD-L1 expression, while one study reported the downregulation of surface PD-L1 [25]. For example, Gong et al reported that paclitaxel induced PD-L1 surface protein and mRNA expression in two different cancer cell models [27]. Similarly, Peng reported that PD-L1 expression in ovarian cancer cell lines was augmented via NF-κB signaling by paclitaxel, gemcitabine or carboplatin treatment [28]. In contrast, Ghebeh *et al*., reported that doxorubicin downregulated the surface expression of PD-L1 in breast cancer cells and upregulated nuclear expression of PD-L1 [26]. One possible explanation for the difference among these previous studies, might be due to differences in the cell lines and anticancer agents used in each study.

In this study, we have tested Abraxane^{TM}, gemcitabine, paclitaxel as well as both solution and nanoemulsion formulation of DHA-SBT-1214, used alone or combined with other agents when treating pancreatic cancer. The concentration of each anticancer agent in our experiments was based on IC_{50} value of Panc02 cells [25, 48, 49]. The respective difference in drug concentration among the anticancer agents have not significantly influenced the degree of PD-L1 induction by

the agents and the PD-L1 surface protein expression was enhanced in response to all anticancer agents as determined by flow cytometry [26]. In regards to the mechanism of PD-L1 regulation, Pardoll reported that innate and adaptive immune resistance are the two general mechanisms by which tumor cells regulate PD-L1 [50]. In general, anticancer agents not only cause cytotoxicity, but also alter the tumor immune response which may induce tumor immune escape. In this study, we demonstrated anti-tumor effects of different anticancer agents in combination to PD-L1 blockade in vivo by using a syngeneic murine pancreas cancer model. It is well known that PD-1/PD-L1 interactions induce a negative regulation, which is critical for immune homeostasis after activation of T-cells [51, 52]. This negative regulation is thought to be beneficial for cancer cells to escape from tumor-specific T-cell immunity [53, 54]. There has also been a study using a pancreatic cancer cell line that showed PD-L1 blocking inhibited tumor development, although these studies have not used anticancer agents along with immune check point inhibitor [14]. In our study, we used a pancreas cancer model established by subcutaneous injection of murine pancreatic cancer cells into the mouse pancreas because cancer immunity is highly regulated by specie-specific leukocyte recruitment. As a result, blocking of PD-L1 reduced rate of tumor growth in our pancreas cancer model when used as a single treatment option or when used in combination with commonly used anticancer agents (Paclitaxel, Abraxane and Gemcitabine) for pancreatic cancer. However, combination of NE-DHA-SBT-1214 with PD-L1 blockade showed significant tumor suppression and kept tumor regressed even after treatment, suggesting that PD-L1 is a possible target for treatment of pancreas cancer.

Freeman *et al*, reported that PD-L1 reduced T-cell proliferation, however we found that the number of tumor-infiltrating cells was increased after anti-PD-L1 antibody treatment. Increase in IFN-gamma by blocking of the PD-1/PD-L1 pathway has been demonstrated in

several models, including chronic infectious diseases, in addition to cancer immunity [55]. Treatment with anti-PD-L1 antibody increased the expression of PD-L1 that might due to increased infiltration of IFN-gamma producing CD8+ cells to tumor tissue. Other possible reason for upregulation of PD-L1 mRNA and protein level after anti-PD-L1 antibody treatment is the recruitment of macrophages and Myeloid derived suppressor cells (MDSC) which also express PD-L1. The increased IFN-gamma from infiltrating CD8+ cells in tumor tissue might contribute to the antitumor effect, because a large amount of IFN-gamma expression from effector T-cells for a long period can induce infiltration of inflammatory cells such as M1 macrophages which enhance anti-tumor immunity [53, 56]. Macrophages in the tumor microenvironment overexpress Arginase-1 indicating that these macrophages are M1 in addition to possible presence of MDSC. Thus, it is conceivable that the suppressive effect of anti-PD-L1 antibody on tumor growth can be mainly explained by the increased number of tumor-infiltrating effector cells in NE-DHA-SBT-1214 combination treatment group. In other words, in untreated group, PD-L1 might attenuate tumor immunity in this cancer model by decreasing the infiltration of IFN-gamma-producing T-cells and M1 macrophages. As same cells that were injected into mice to form a pancreatic tumor expressed very high level of PD-L1 after IFN-gamma treatment in vitro. In our study, the number of tumor-infiltrating CD4+ T-cells did not decrease after PD-L1 blockade. Taken together, the results suggested that PD-L1 blockade can decrease the pancreatic tumor burden through synergic effect of NE-DHA-SBT-1214. Furthermore, histology of tumor tissues from different treatment groups showed that tumor from NE-DHA-SBT-1214 treated group has less dense stroma compared to solid tumor mass from other treatment groups. However, neither single nor the combination therapy of most commonly used anticancer agents unexpectedly did not show an additive anti-tumor effect except NE-DHA-SBT-1214. One possible explanation for

better efficacy of NE-DHA-SBT-1214 is its role in treating cancer stem cells as compared to other anti-cancer agents.

CONCLUSIONS

The results of this study indicate a significant tumor growth suppression by blocking PD-L1 in combination to NE-DHA-SBT-1214. Blockade of PD-L1 increased intra-tumoral IFN-gamma producing T-cells and infiltration of inflammatory macrophages, which might directly lead to the anti-tumor effect. In contrast, both PD-1 and PD-L1 levels were high in combination of commonly used anti-cancer agents emphasizing increased tumor infiltration of Treg cells, which might be primarily responsible for the non-anti-tumor effect. These differential roles of different anticancer agent combinations may be a good start to explore other clinical treatments options for pancreatic cancers. Overall, we believe that the data provided in the present study, may aid in the design of more effective treatments that combine chemotherapy and immunotherapy.

ACKNOWLEDGEMENTS

Financial support was provided by the National Cancer Institute of the National Institutes of Health through contract and grants HHSN261201500018C (to JE) and R21-CA179652 (to MA) and R21-CA213114 (to MA and GGM). Additionally, transmission electron microscopy of the nanoemulsion samples was performed by Mr. William Fowle at the Electron Microscopy Center, Northeastern University (Boston, MA). Lastly, we deeply appreciate the assistance of Dr. Ahmed Radwan, a research fellow in Dr. Ali Hafezi-Mogadham's laboratory in the Department

of Radiology at the Brigham and Women's Hospital (Boston, MA) for assistance with microscopic visualization of IHC slides.

REFERENCES

1. Siegel RL, Miller KD, Jemal A. Cancer statistics, 2015. *CA Cancer J Clin* 2015;**65**: 5-29.
2. Mazur PK, Siveke JT. Genetically engineered mouse models of pancreatic cancer: unravelling tumour biology and progressing translational oncology. *Gut* 2012;**61**: 1488-500.
3. Dorado J, Lonardo E, Miranda-Lorenzo I, Heeschen C. Pancreatic cancer stem cells: new insights and perspectives. *J Gastroenterol* 2011;**46**: 966-73.
4. Vredenburg MR, Ojima I, Veith J, Pera P, Kee K, Cabral F, Sharma A, Kanter P, Greco WR, Bernacki RJ. Effects of orally active taxanes on P-glycoprotein modulation and colon and breast carcinoma drug resistance. *Journal of the National Cancer Institute* 2001;**93**: 1234-45.
5. Von Hoff DD, Ervin T, Arena FP, Chiorean EG, Infante J, Moore M, Seay T, Tjulandin SA, Ma WW, Saleh MN, Harris M, Reni M, et al. Increased survival in pancreatic cancer with nab-paclitaxel plus gemcitabine. *N Engl J Med* 2013;**369**: 1691-703.
6. Hutchinson L, Kirk R. High drug attrition rates--where are we going wrong? *Nature reviews Clinical oncology* 2011;**8**: 189-90.
7. Ojima I, Chen J, Sun L, Borella CP, Wang T, Miller ML, Lin S, Geng X, Kuznetsova L, Qu C, Gallager D, Zhao X, et al. Design, synthesis, and biological evaluation of new-generation taxoids. *J Med Chem* 2008;**51**: 3203-21.
8. Botchkina GI, Zuniga ES, Das M, Wang Y, Wang H, Zhu S, Savitt AG, Rowehl RA, Leyfman Y, Ju J, Shroyer K, Ojima I. New-generation taxoid SB-T-1214 inhibits stem cell-related gene expression in 3D cancer spheroids induced by purified colon tumor-initiating cells. *Molecular cancer* 2010;**9**: 192.
9. Das M, Zuniga E, Ojima I. Novel Taxoid-Based Tumor-Targeting Drug Conjugates. *Chim Oggi* 2009;**27**: 54-6.
10. Kuznetsova L, Chen J, Sun L, Wu X, Pepe A, Veith JM, Pera P, Bernacki RJ, Ojima I. Syntheses and evaluation of novel fatty acid-second-generation taxoid conjugates as promising anticancer agents. *Bioorganic & medicinal chemistry letters* 2006;**16**: 974-7.
11. Ahmad G, El Sadda R, Botchkina G, Ojima I, Egan J, Amiji M. Nanoemulsion formulation of a novel taxoid DHA-SBT-1214 inhibits prostate cancer stem cell-induced tumor growth. *Cancer letters* 2017;**406**: 71-80.
12. Couzin-Frankel J. Breakthrough of the year 2013. Cancer immunotherapy. *Science* 2013;**342**: 1432-3.
13. Brahmer JR, Hammers H, Lipson EJ. Nivolumab: targeting PD-1 to bolster antitumor immunity. *Future Oncol* 2015;**11**: 1307-26.
14. Nomi T, Sho M, Akahori T, Hamada K, Kubo A, Kanehiro H, Nakamura S, Enomoto K, Yagita H, Azuma M, Nakajima Y. Clinical significance and therapeutic potential of the programmed death-1 ligand/programmed death-1 pathway in human pancreatic cancer.

Clinical cancer research : an official journal of the American Association for Cancer Research 2007;**13**: 2151-7.

15. Brahmer J, Reckamp KL, Baas P, Crino L, Eberhardt WE, Poddubskaya E, Antonia S, Pluzanski A, Vokes EE, Holgado E, Waterhouse D, Ready N, et al. Nivolumab versus Docetaxel in Advanced Squamous-Cell Non-Small-Cell Lung Cancer. *N Engl J Med* 2015;**373**: 123-35.
16. Larkin J, Hodi FS, Wolchok JD. Combined Nivolumab and Ipilimumab or Monotherapy in Untreated Melanoma. *N Engl J Med* 2015;**373**: 1270-1.
17. Motzer RJ, Rini BI, McDermott DF, Redman BG, Kuzel TM, Harrison MR, Vaishampayan UN, Drabkin HA, George S, Logan TF, Margolin KA, Plimack ER, et al. Nivolumab for Metastatic Renal Cell Carcinoma: Results of a Randomized Phase II Trial. *Journal of clinical oncology : official journal of the American Society of Clinical Oncology* 2015;**33**: 1430-7.
18. Jiang C, Cai X, Zhang H, Xia X, Zhang B, Xia L. Activity and Immune Correlates of a Programmed Death-1 Blockade Antibody in the treatment of Refractory Solid Tumors. *J Cancer* 2018;**9**: 205-12.
19. Torphy RJ, Schulick RD, Zhu Y. Newly Emerging Immune Checkpoints: Promises for Future Cancer Therapy. *Int J Mol Sci* 2017;**18**.
20. They L, Michaud HA, Becquart O, Lafont V, Guillot B, Boissiere-Michot F, Jarlier M, Mollevi C, Eliaou JF, Bonnefoy N, Gros L. PD-1 blockade at the time of tumor escape potentiates the immune-mediated antitumor effects of a melanoma-targeting monoclonal antibody. *Oncoimmunology* 2017;**6**: e1353857.
21. Okudaira K, Hokari R, Tsuzuki Y, Okada Y, Komoto S, Watanabe C, Kurihara C, Kawaguchi A, Nagao S, Azuma M, Yagita H, Miura S. Blockade of B7-H1 or B7-DC induces an anti-tumor effect in a mouse pancreatic cancer model. *Int J Oncol* 2009;**35**: 741-9.
22. Brahmer JR, Tykodi SS, Chow LQ, Hwu WJ, Topalian SL, Hwu P, Drake CG, Camacho LH, Kauh J, Odunsi K, Pitot HC, Hamid O, et al. Safety and activity of anti-PD-L1 antibody in patients with advanced cancer. *N Engl J Med* 2012;**366**: 2455-65.
23. Le DT, Lutz E, Uram JN, Sugar EA, Onners B, Solt S, Zheng L, Diaz LA, Jr., Donehower RC, Jaffee EM, Laheru DA. Evaluation of ipilimumab in combination with allogeneic pancreatic tumor cells transfected with a GM-CSF gene in previously treated pancreatic cancer. *J Immunother* 2013;**36**: 382-9.
24. Lutz ER, Wu AA, Bigelow E, Sharma R, Mo G, Soares K, Solt S, Dorman A, Wamwea A, Yager A, Laheru D, Wolfgang CL, et al. Immunotherapy converts nonimmunogenic pancreatic tumors into immunogenic foci of immune regulation. *Cancer Immunol Res* 2014;**2**: 616-31.
25. Zhang P, Su DM, Liang M, Fu J. Chemopreventive agents induce programmed death-1-ligand 1 (PD-L1) surface expression in breast cancer cells and promote PD-L1-mediated T cell apoptosis. *Mol Immunol* 2008;**45**: 1470-6.
26. Ghebeh H, Lehe C, Barhoush E, Al-Romaih K, Tulbah A, Al-Alwan M, Hendrayani SF, Manogaran P, Alaiya A, Al-Tweigeri T, Aboussekhra A, Dermime S. Doxorubicin downregulates cell surface B7-H1 expression and upregulates its nuclear expression in breast cancer cells: role of B7-H1 as an anti-apoptotic molecule. *Breast cancer research : BCR* 2010;**12**: R48.

27. Gong W, Song Q, Lu X, Gong W, Zhao J, Min P, Yi X. Paclitaxel induced B7-H1 expression in cancer cells via the MAPK pathway. *J Chemother* 2011;**23**: 295-9.
28. Peng J, Hamanishi J, Matsumura N, Abiko K, Murat K, Baba T, Yamaguchi K, Horikawa N, Hosoe Y, Murphy SK, Konishi I, Mandai M. Chemotherapy Induces Programmed Cell Death-Ligand 1 Overexpression via the Nuclear Factor-kappaB to Foster an Immunosuppressive Tumor Microenvironment in Ovarian Cancer. *Cancer research* 2015;**75**: 5034-45.
29. Ojima I, Wang T, Miller ML, Lin S, Borella CP, Geng X, Pera P, Bernacki RJ. Synthesis and structure-activity relationships of new second-generation taxoids. *Bioorg Med Chem Lett* 1999;**9**: 3423-8.
30. Ojima I, Slater JC, Michaud E, Kuduk SD, Bounaud PY, Vrignaud P, Bissery MC, Veith JM, Pera P, Bernacki RJ. Syntheses and structure-activity relationships of the second-generation antitumor taxoids: exceptional activity against drug-resistant cancer cells. *J Med Chem* 1996;**39**: 3889-96.
31. Shah L, Gattacceca F, Amiji MM. CNS delivery and pharmacokinetic evaluations of DALDA analgesic peptide analog administered in Nano-sized oil-in-water emulsion formulation. *Pharmaceutical research* 2014;**31**: 1315-24.
32. Kadakia E, Shah L, Amiji MM. Mathematical Modeling and Experimental Validation of Nanoemulsion-Based Drug Transport across Cellular Barriers. *Pharmaceutical research* 2017;**34**: 1416-27.
33. Ganta S, Singh A, Rawal Y, Cacaccio J, Patel NR, Kulkarni P, Ferris CF, Amiji MM, Coleman TP. Formulation development of a novel targeted theranostic nanoemulsion of docetaxel to overcome multidrug resistance in ovarian cancer. *Drug Deliv* 2016;**23**: 968-80.
34. Morikane K, Tempero RM, Sivinski CL, Nomoto M, Van Lith ML, Muto T, Hollingsworth MA. Organ-specific pancreatic tumor growth properties and tumor immunity. *Cancer Immunol Immunother* 1999;**47**: 287-96.
35. English K, Barry FP, Field-Corbett CP, Mahon BP. IFN-gamma and TNF-alpha differentially regulate immunomodulation by murine mesenchymal stem cells. *Immunol Lett* 2007;**110**: 91-100.
36. Kee JY, Ito A, Hojo S, Hashimoto I, Igarashi Y, Tsukada K, Irimura T, Shibahara N, Nakayama T, Yoshie O, Sakurai H, Saiki I, et al. Chemokine CXCL16 suppresses liver metastasis of colorectal cancer via augmentation of tumor-infiltrating natural killer T cells in a murine model. *Oncology reports* 2013;**29**: 975-82.
37. Chauhan P, Hu S, Sheng WS, Prasad S, Lokensgard JR. Modulation of Microglial Cell Fcgamma Receptor Expression Following Viral Brain Infection. *Scientific reports* 2017;**7**: 41889.
38. Allie N, Grivennikov SI, Keeton R, Hsu NJ, Bourigault ML, Court N, Fremond C, Yeremeev V, Shebzukhov Y, Ryffel B, Nedospasov SA, Quesniaux VF, et al. Prominent role for T cell-derived tumour necrosis factor for sustained control of Mycobacterium tuberculosis infection. *Scientific reports* 2013;**3**: 1809.
39. Sarker DK. Engineering of nanoemulsions for drug delivery. *Current drug delivery* 2005;**2**: 297-310.
40. Lu C, Paschall AV, Shi H, Savage N, Waller JL, Sabbatini ME, Oberlies NH, Pearce C, Liu K. The MLL1-H3K4me3 Axis-Mediated PD-L1 Expression and Pancreatic Cancer Immune Evasion. *Journal of the National Cancer Institute* 2017;**109**.

41. Lu C, Talukder A, Savage NM, Singh N, Liu K. JAK-STAT-mediated chronic inflammation impairs cytotoxic T lymphocyte activation to decrease anti-PD-1 immunotherapy efficacy in pancreatic cancer. *Oncoimmunology* 2017;**6**: e1291106.
42. Maude SL, Frey N, Shaw PA, Aplenc R, Barrett DM, Bunin NJ, Chew A, Gonzalez VE, Zheng Z, Lacey SF, Mahnke YD, Melenhorst JJ, et al. Chimeric antigen receptor T cells for sustained remissions in leukemia. *N Engl J Med* 2014;**371**: 1507-17.
43. Rowinsky EK. The development and clinical utility of the taxane class of antimicrotubule chemotherapy agents. *Annu Rev Med* 1997;**48**: 353-74.
44. McGuire WP, Rowinsky EK, Rosenshein NB, Grumbine FC, Ettinger DS, Armstrong DK, Donehower RC. Taxol: a unique antineoplastic agent with significant activity in advanced ovarian epithelial neoplasms. *Ann Intern Med* 1989;**111**: 273-9.
45. Schiff PB, Horwitz SB. Taxol stabilizes microtubules in mouse fibroblast cells. *Proc Natl Acad Sci U S A* 1980;**77**: 1561-5.
46. Jordan MA, Toso RJ, Thrower D, Wilson L. Mechanism of mitotic block and inhibition of cell proliferation by taxol at low concentrations. *Proc Natl Acad Sci U S A* 1993;**90**: 9552-6.
47. Rossi J, Giasson S, Khalid MN, Delmas P, Allen C, Leroux JC. Long-circulating poly(ethylene glycol)-coated emulsions to target solid tumors. *Eur J Pharm Biopharm* 2007;**67**: 329-38.
48. Sakai H, Kokura S, Ishikawa T, Tsuchiya R, Okajima M, Matsuyama T, Adachi S, Katada K, Kamada K, Uchiyama K, Handa O, Takagi T, et al. Effects of anticancer agents on cell viability, proliferative activity and cytokine production of peripheral blood mononuclear cells. *J Clin Biochem Nutr* 2013;**52**: 64-71.
49. Okino H, Maeyama R, Manabe T, Matsuda T, Tanaka M. Trans-tissue, sustained release of gemcitabine from photocured gelatin gel inhibits the growth of heterotopic human pancreatic tumor in nude mice. *Clinical cancer research : an official journal of the American Association for Cancer Research* 2003;**9**: 5786-93.
50. Pardoll DM. The blockade of immune checkpoints in cancer immunotherapy. *Nature reviews Cancer* 2012;**12**: 252-64.
51. Nishimura H, Honjo T. PD-1: an inhibitory immunoreceptor involved in peripheral tolerance. *Trends Immunol* 2001;**22**: 265-8.
52. Okazaki T, Maeda A, Nishimura H, Kurosaki T, Honjo T. PD-1 immunoreceptor inhibits B cell receptor-mediated signaling by recruiting src homology 2-domain-containing tyrosine phosphatase 2 to phosphotyrosine. *Proc Natl Acad Sci U S A* 2001;**98**: 13866-71.
53. Iwai Y, Terawaki S, Honjo T. PD-1 blockade inhibits hematogenous spread of poorly immunogenic tumor cells by enhanced recruitment of effector T cells. *Int Immunol* 2005;**17**: 133-44.
54. Hirano F, Kaneko K, Tamura H, Dong H, Wang S, Ichikawa M, Rietz C, Flies DB, Lau JS, Zhu G, Tamada K, Chen L. Blockade of B7-H1 and PD-1 by monoclonal antibodies potentiates cancer therapeutic immunity. *Cancer research* 2005;**65**: 1089-96.
55. Lukens JR, Cruise MW, Lassen MG, Hahn YS. Blockade of PD-1/B7-H1 interaction restores effector CD8+ T cell responses in a hepatitis C virus core murine model. *J Immunol* 2008;**180**: 4875-84.
56. Guiducci C, Vicari AP, Sangaletti S, Trinchieri G, Colombo MP. Redirecting in vivo elicited tumor infiltrating macrophages and dendritic cells towards tumor rejection. *Cancer research* 2005;**65**: 3437-46.

FIGURE LEGEND

Figure 1. (A) – Transmission electron microscopy image of DHA-SBT-1214 encapsulated of nanoemulsion. **(B)** – The oil droplet particle size determination in nm. **(C)** – The measurement of zeta potential or surface charge on the oil droplets in mV; and **(D)** – The uptake of rhodamine-encapsulated nanoemulsion formulation in Panc02 cells. Fluorescence microscopy images showing the blue (nucleus), red (rhodamine encapsulated nanoemulsion) and overlay images in purple color. The images were acquired at 63x magnification. The image scale bar is 100 µm.

Figure 2. The activity of different anti-cancer agents against Panc02 cells *in vitro*. The percentage maximal response as a function of anti-cancer agents when administered to Panc02 cells. The cell viability was measured using the 3-(4,5-dimethylthiazol-2-yl)-2,5-diphenyltetrazolium bromide (MTT) assay after 96 h of incubation at 37 ºC. Data represent mean ± standard deviation (n=3). Significant differences are indicated as follows: *p < 0.05, and **p < 0.01.

Figure 3. *In vivo* efficacy of the PD-L1 antibody in combination to different therapeutic drugs including gemcitabine solution, Abraxane™ paclitaxel in solution, DHA-SBT-1214 in solution and NE-DHA-SBT-1214 against Panc02 induced syngeneic mice tumors. **(A)**– Graph summarizing all treatment modalities. The values are means ± SD (n=3). Significant differences are indicated as follows: *p < 0.05, and **p< 0.01. **(B)**– Tumor images taken at the time of harvest from different treatment modalities. **(3b-A)**– Tumors from mice treated with vehicle; **(3b-B)**– Three tumors each from PD-L1 (200µg) treated mice; **(3b-C, D)**–Tumors from Abraxane™ plus IgG or PD-L1 (200µg) treated mice respectively; **(3b-E)**– Tumors from NE-DHA-SBT-1214 (10mg/kg) plus IgG (200µg) treated mice; **(3b-F, G)**– Tumors from gemcitabine plus IgG or PD-L1 (200µg) treated mice respectively; **(3b-H)**– Tumors from NE-DHA-SBT-1214 (10mg/kg) plus PD-L1 (200µg) treated mice; **(3b-I, J)**– Tumors from NE-DHA-SBT-1214 (25mg/kg) plus IgG or PD-L1 (200µg) treated mice respectively. **(C)**– Graph for all the tumors from **(3B)** to show their progression over time.

Figure 4. *In vivo* PD-L1 surface protein expression in response to different therapeutic modalities. **(A)**– mRNA expression of PD-L1 from different mouse tumor treatment groups analyzed using RT-PCR. Relative gene expression for RT-PCR data was calculated relative to murine β-actin. **(B)**– Tumor Tissue lysate from different treated groups was prepared and protein level of different proteins was analyzed using western blotting. **(C)**– The bands corresponding to PD-L1 were quantified using Image J software and was normalized relative to band intensities for the corresponding Histone 3 loading controls. The bar represent the mean ± standard deviation of data from at least 3 independent experiments; *p<0.05, **p<0.01.

Figure 5. Histopathological evaluation of the Panc02-induced tumor tissues collected from control and different combination treated mice (hematoxylin & eosin staining). Significant reduction in tumor stroma observed with combination NE-DHA-SBT-1214 and anti-PD-L1 treated groups. The images were taken at 63x magnification.

Figure 6. Immunohistochemical analysis of infiltrating CD4 or CD8 cells by immunohistochemistry and their quantification. **(A & Supplementary Figure 3A)**–Tumor

Tissue from all treatments groups were fixed in PFA and stained with anti-CD4 antibody, **(B & Supplementary Figure 3B)**– anti-CD8 antibody, and **(C & Supplementary Figure 3C)**– anti-PD1 antibody according to vendors protocol. The images were taken at 63x magnification.

Figure 1.

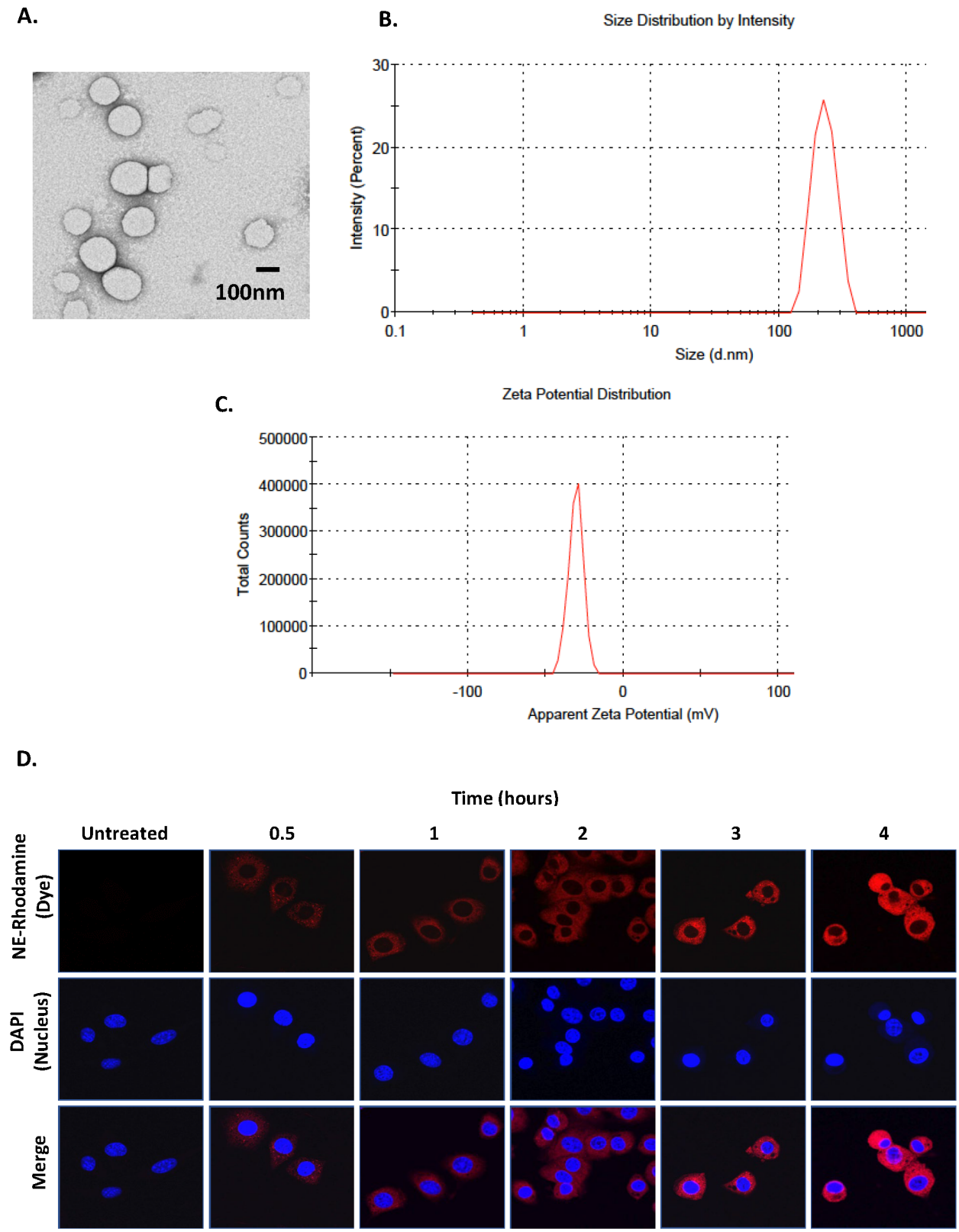
A.
100nm
B.
Size Distribution by Intensity
Intensity (Percent)
30
20
10
0
0.1
1
10
100
1000
Size (d.nm)
C.
Zeta Potential Distribution
Total Counts
500000
400000
300000
200000
100000
0
-100
0
100
Apparent Zeta Potential (mV)
D.
Time (hours)
Untreated
0.5
1
2
3
4
NE-Rhodamine (Dye)
DAPI (Nucleus)
Merge

Figure 2.

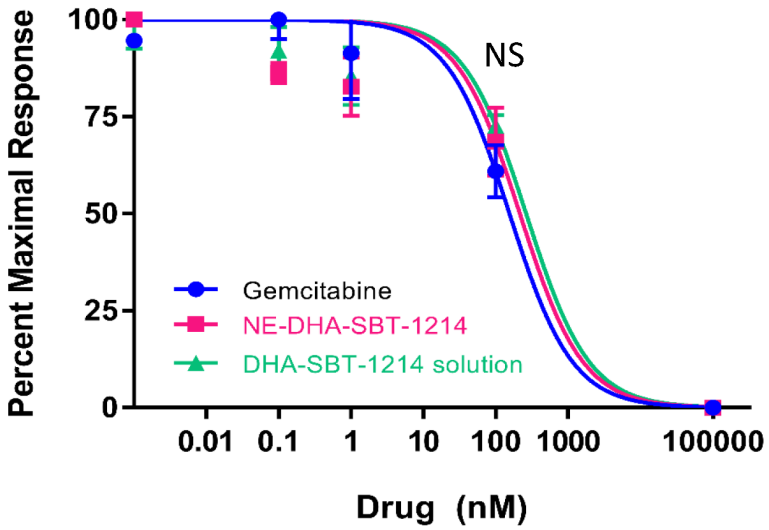

Drug	IC50 (nM) (±S.D.)	P-value
Gemcitabine	154.6 ± 63.2	-
NE-DHA-SBT-1214	215.1 ± 96.5	0.373
DHA-SBT-1214 solution	262.8 ± 34.8	0.0930

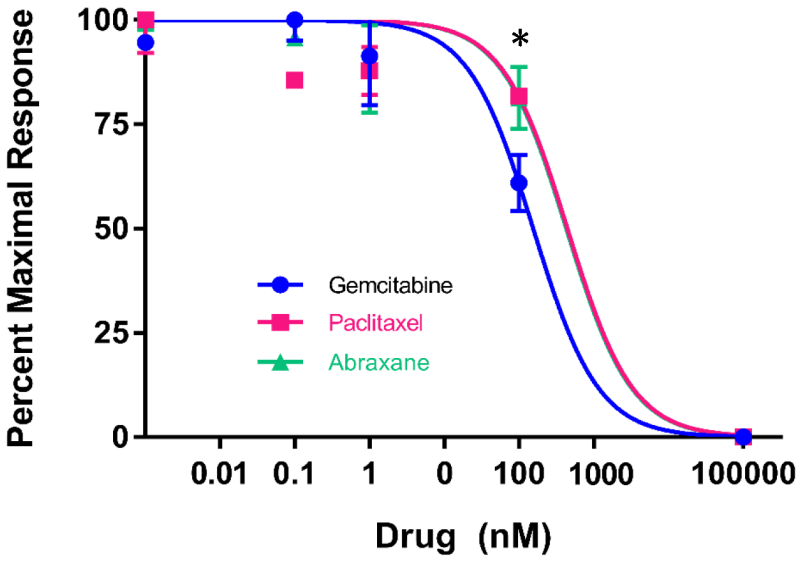

Drug	IC50 (nM) (±S.D.)	P-value
Gemcitabine	154.6 ± 63.2	-
Paclitaxel	443.9 ± 183.0	0.0459
Abraxane	428.2 ± 163.8	0.0501

Figure 3.

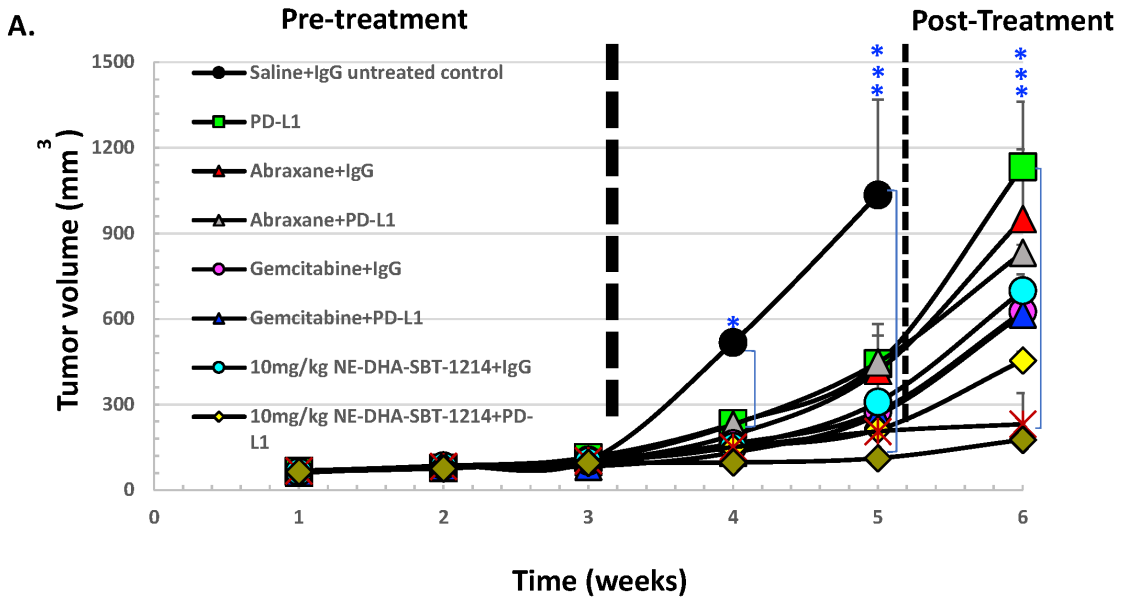
A.
Pre-treatment
Post-Treatment
Saline+IgG untreated control
PD-L1
Abraxane+IgG
Abraxane+PD-L1
Gemcitabine+IgG
Gemcitabine+PD-L1
10mg/kg NE-DHA-SBT-1214+IgG
10mg/kg NE-DHA-SBT-1214+PD-L1
Tumor volume (mm 3)
Time (weeks)

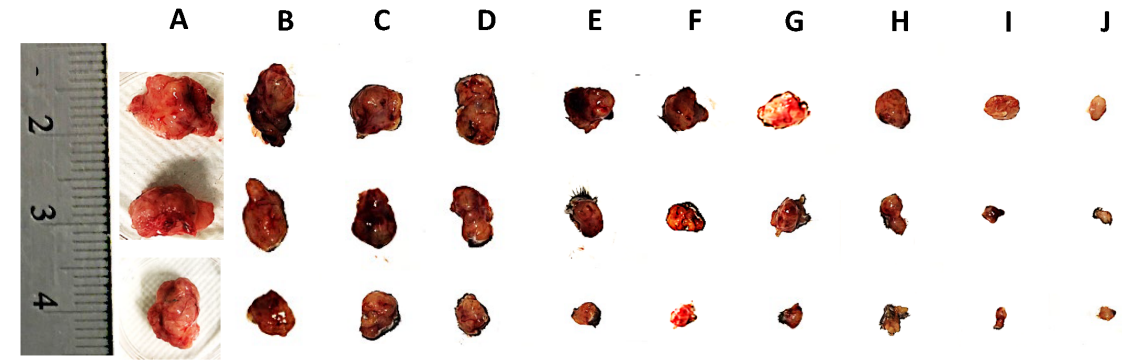
B.
A
B
C
D
E
F
G
H
I
J

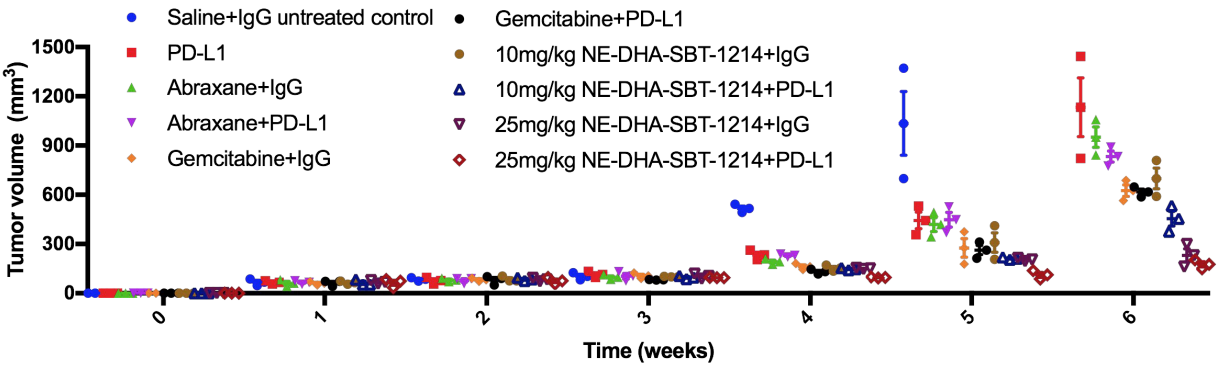
C.
Saline+IgG untreated control
PD-L1
Abraxane+IgG
Abraxane+PD-L1
Gemcitabine+IgG
Gemcitabine+PD-L1
10mg/kg NE-DHA-SBT-1214+IgG
10mg/kg NE-DHA-SBT-1214+PD-L1
25mg/kg NE-DHA-SBT-1214+IgG
25mg/kg NE-DHA-SBT-1214+PD-L1
Tumor volume (mm3)
Time (weeks)

Figure 4.

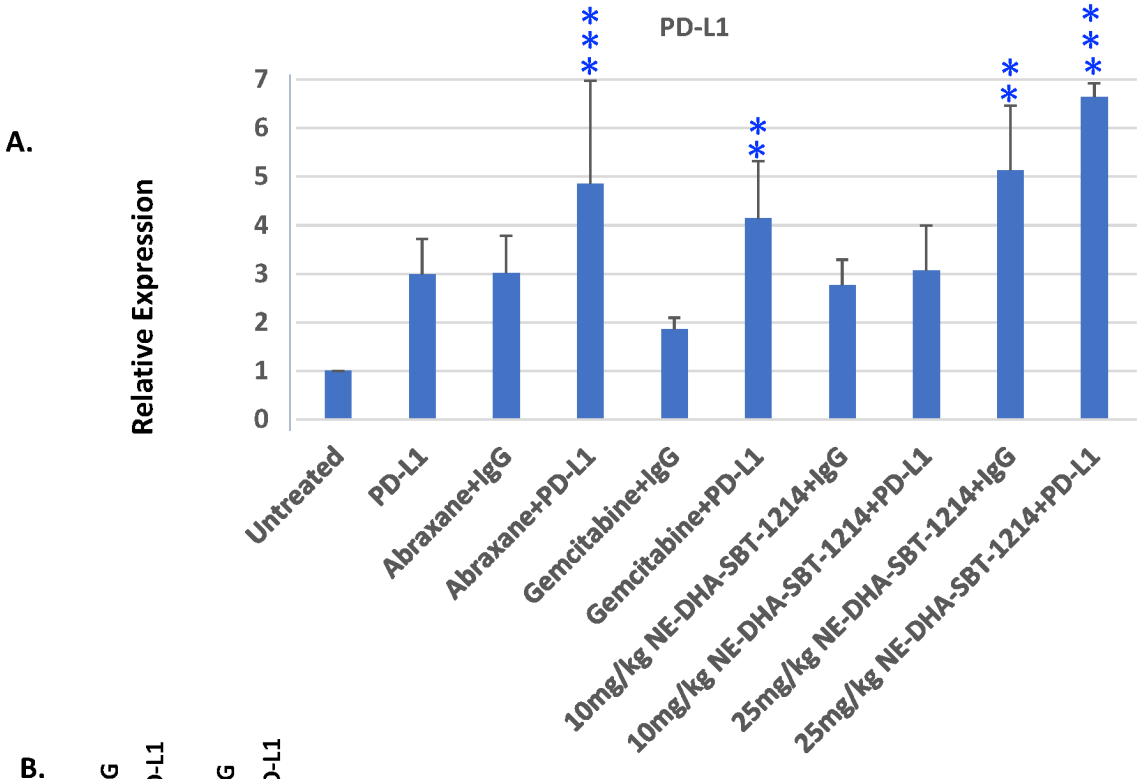
A.
PD-L1
Relative Expression
0
1
2
3
4
5
6
7
Untreated
PD-L1
Abraxane+IgG
Abraxane+PD-L1
Gemcitabine+IgG
Gemcitabine+PD-L1
10mg/kg NE-DHA-SBT-1214+IgG
10mg/kg NE-DHA-SBT-1214+PD-L1
25mg/kg NE-DHA-SBT-1214+IgG
25mg/kg NE-DHA-SBT-1214+PD-L1

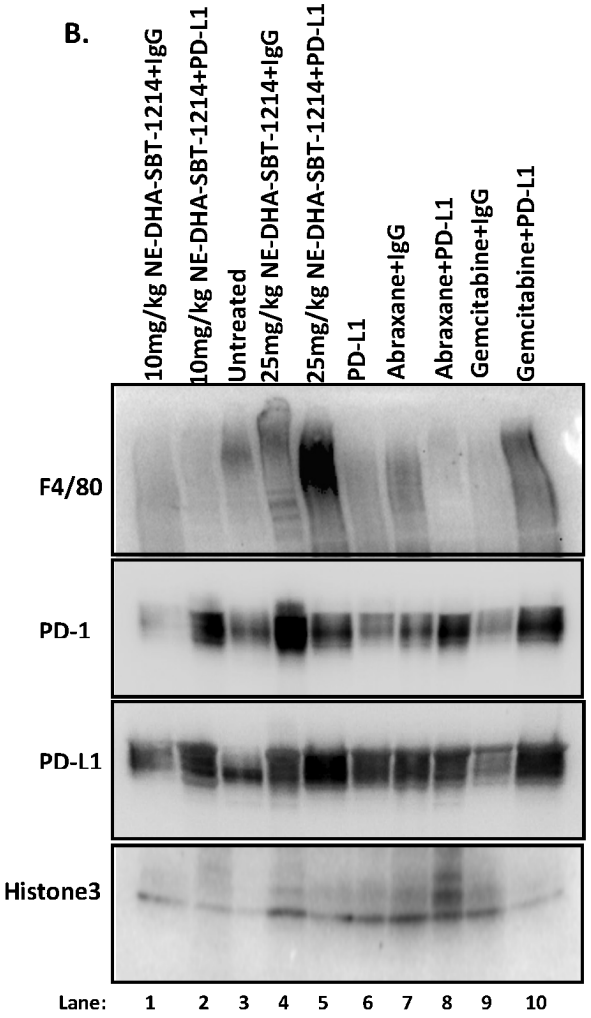
B.
10mg/kg NE-DHA-SBT-1214+IgG
10mg/kg NE-DHA-SBT-1214+PD-L1
Untreated
25mg/kg NE-DHA-SBT-1214+IgG
25mg/kg NE-DHA-SBT-1214+PD-L1
PD-L1
Abraxane+IgG
Abraxane+PD-L1
Gemcitabine+IgG
Gemcitabine+PD-L1
F4/80
PD-1
PD-L1
Histone3
Lane: 1 2 3 4 5 6 7 8 9 10
Drug Treatment

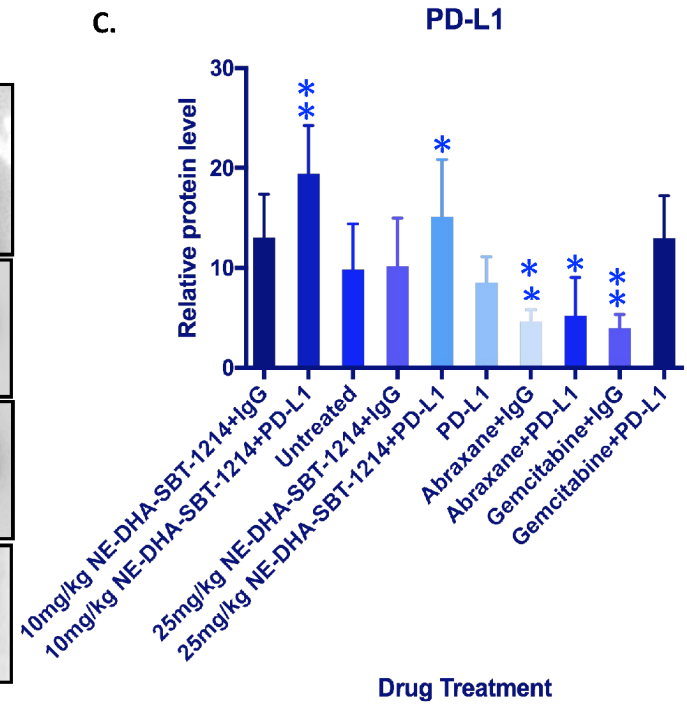
C.
PD-L1
Relative protein level
0
10
20
30
10mg/kg NE-DHA-SBT-1214+IgG
10mg/kg NE-DHA-SBT-1214+PD-L1
Untreated
25mg/kg NE-DHA-SBT-1214+IgG
25mg/kg NE-DHA-SBT-1214+PD-L1
PD-L1
Abraxane+IgG
Abraxane+PD-L1
Gemcitabine+IgG
Gemcitabine+PD-L1
Drug Treatment

Figure 5.

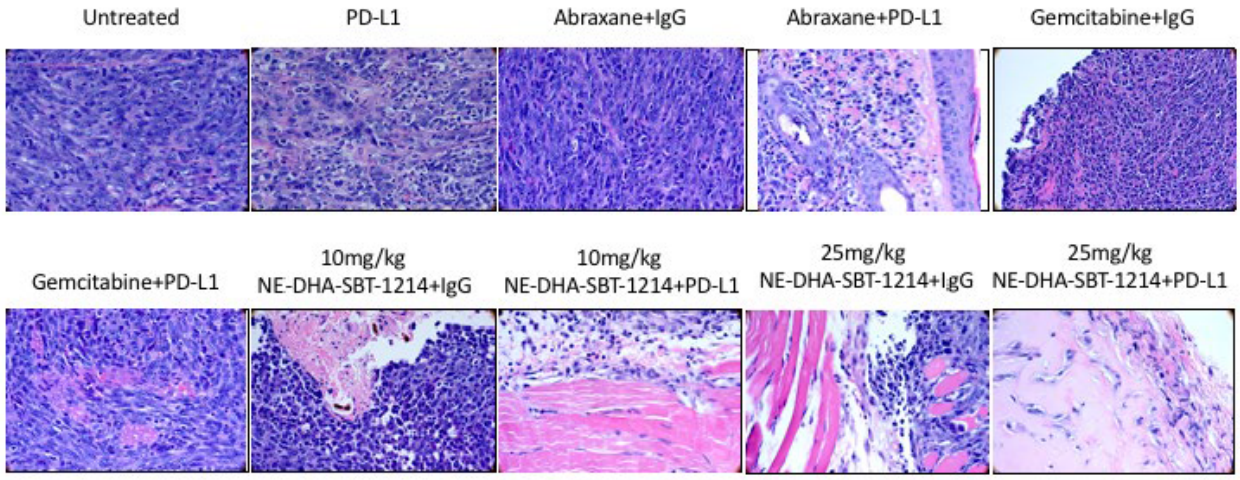
Untreated
PD-L1
Abraxane+IgG
Abraxane+PD-L1
Gemcitabine+IgG
Gemcitabine+PD-L1
10mg/kg
NE-DHA-SBT-1214+IgG
10mg/kg
NE-DHA-SBT-1214+PD-L1
25mg/kg
NE-DHA-SBT-1214+IgG
25mg/kg
NE-DHA-SBT-1214+PD-L1

Figure 6.

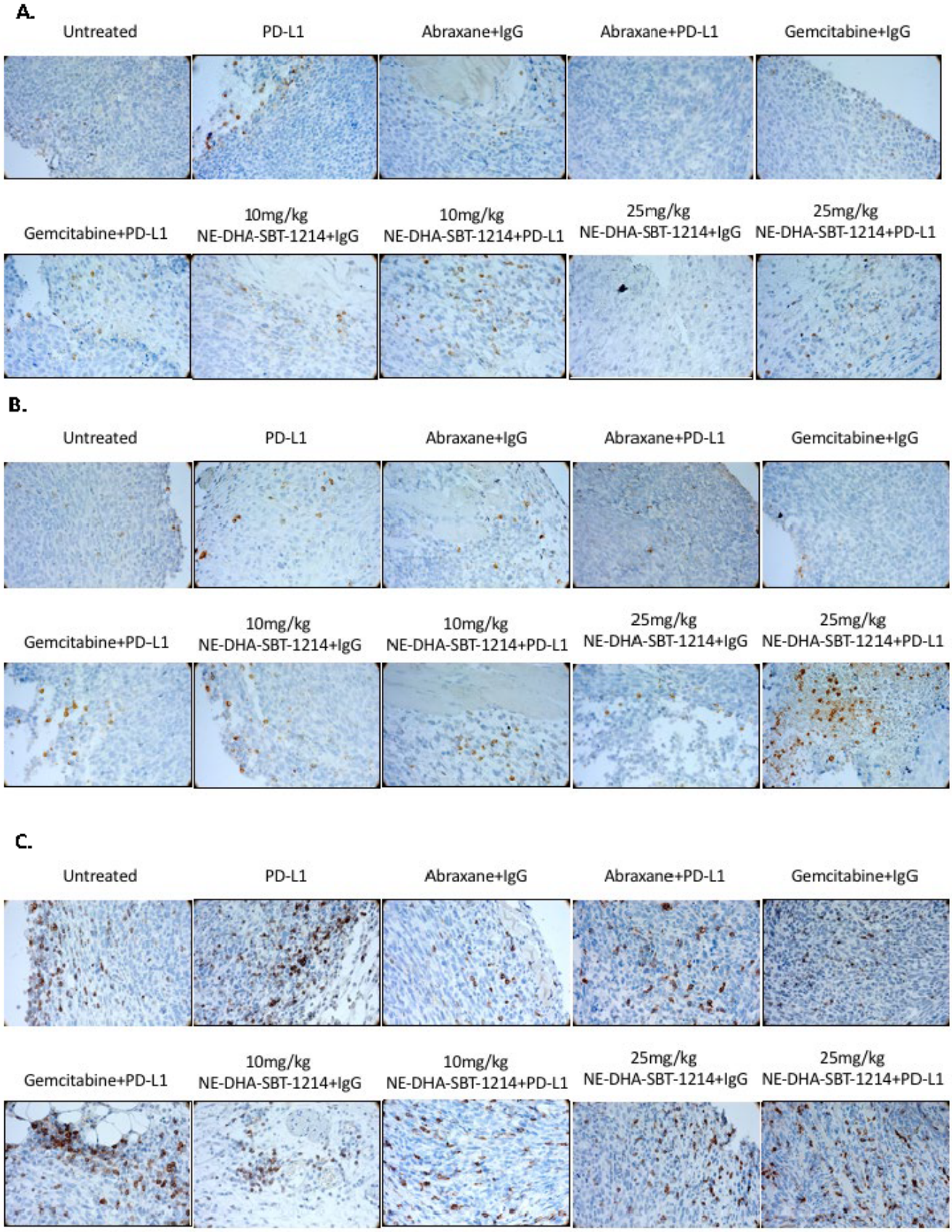
A.
Untreated
PD-L1
Abraxane+IgG
Abraxane+PD-L1
Gemcitabine+IgG
Gemcitabine+PD-L1
10mg/kg NE-DHA-SBT-1214+IgG
10mg/kg NE-DHA-SBT-1214+PD-L1
25mg/kg NE-DHA-SBT-1214+IgG
25mg/kg NE-DHA-SBT-1214+PD-L1
B.
Untreated
PD-L1
Abraxane+IgG
Abraxane+PD-L1
Gemcitabine+IgG
Gemcitabine+PD-L1
10mg/kg NE-DHA-SBT-1214+IgG
10mg/kg NE-DHA-SBT-1214+PD-L1
25mg/kg NE-DHA-SBT-1214+IgG
25mg/kg NE-DHA-SBT-1214+PD-L1
C.
Untreated
PD-L1
Abraxane+IgG
Abraxane+PD-L1
Gemcitabine+IgG
Gemcitabine+PD-L1
10mg/kg NE-DHA-SBT-1214+IgG
10mg/kg NE-DHA-SBT-1214+PD-L1
25mg/kg NE-DHA-SBT-1214+IgG
25mg/kg NE-DHA-SBT-1214+PD-L1